§2. Density Limit Studies in LHD

Peterson, B.J., Miyazawa, J., Nishimura, K. (NIFS)

The operational density limit in stellarators is not determined by major disruption and MARFE as in tokamaks, nor is the Greenwald limit directly applicable to net-current free plasmas. Previous investigations [1] have shown that the density in LHD is limited by a radiative thermal instability which results in the collapse of the plasma at a limit which is 1.4 times the previously obtained Sudo limit [2]. In the latest experimental campaign in the Large Helical Device (LHD), line-averaged densities of up to $1.6 \times 10^{20}\mathrm{m}^{-3}$ have been sustained for more than 0.7 s by 11 MW neutral beam injection, which is 1.36 times Sudo scaling. In addition, using multiple hydrogen pellets, the density has been increased to over $2 \times 10^{20}\mathrm{m}^{-3}$ transiently. Also, after boronization of the vacuum vessel wall, indeed, radiation loss, P_{rad}, decreases about 20 ~ 50 %, compared at similar density and input power, P_{abs}, and the density limit increases 20 ~ 50 %. These results indicate the importance of P_{rad} on density limit studies. However, the thermal instability is sometimes triggered even when P_{rad} is less than a half of P_{abs}. These observations call for the investigation of the role of P_{rad} and the exploration of the mechanism which triggers or enhances the thermal instability.

The terminal phase of a typical discharge with radiative collapse is shown in Fig. 1. During the steady state portion of the discharge prior to 2 s, the radiation is proportional to the line-averaged density, $\bar{n}_{\mathrm{e}}$. This phase ends when the radiative thermal instability is triggered as indicated by the sharp increases in P_{rad} and the light impurities emission. At the critical time (t_{c} = 2.1 s in Fig. 1), where P_{rad} is proportional to $\bar{n}_{\mathrm{e}}^{\,3}$ (see Fig. 1(e), where $x = (P_{\mathrm{rad}}'/P_{\mathrm{rad}}) / (\bar{n}_{\mathrm{e}}'/\bar{n}_{\mathrm{e}})$ indicates the power scaling of P_{rad} on the line-averaged density, $\bar{n}_{\mathrm{e}}$) the edge (at $\rho = r/a = 0.9$) temperature decreases to about 150 eV. This characteristic edge temperature is insensitive to P_{abs} and $\bar{n}_{\mathrm{e}}$ as can be seen in Figure 2, and is also observed at both R=3.6 and 3.75 m as long as the wall condition is maintained, confirming that the onset of the thermal instability is closely tied to the edge plasma temperature. After t_{c} the temperature at ρ = 1 has dropped below the measurable limit of 50 eV, which is the temperature below which the oxygen radiation grows rapidly leading to the onset of the radiative thermal instability as seen in Fig. 1(c) followed ~ 50 ms later by $\mathrm{C_{III}}$ which becomes unstable at a lower electron temperature. The radiation is also enhanced after t_{c} as the hot plasma column shrinks leaving an increasingly larger volume of low temperature plasma in which the light impurities radiate strongly. After t_{c} the edge temperature decreases faster than that at core (Fig. 1(d)), presumably due to radiative cooling in the edge by light impurities. Comparison of the growth rate of the $\mathrm{O_V}$ radiation in Fig. 1(c) with the decay rate of the stored energy in Fig. 1(a) also indicates that the radiative thermal instability is responsible for the confinement degradation.

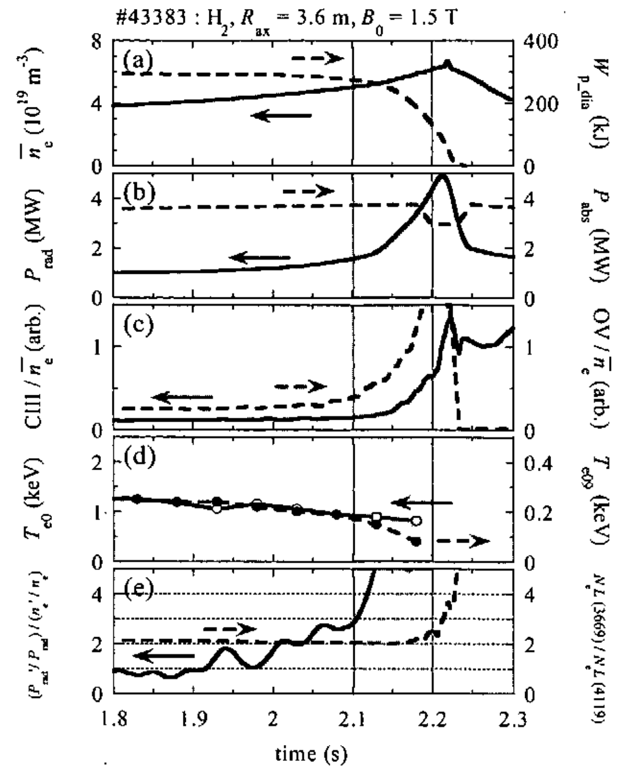

Fig. 1 Typical waveforms of a discharge terminated by radiative collapse in LHD.

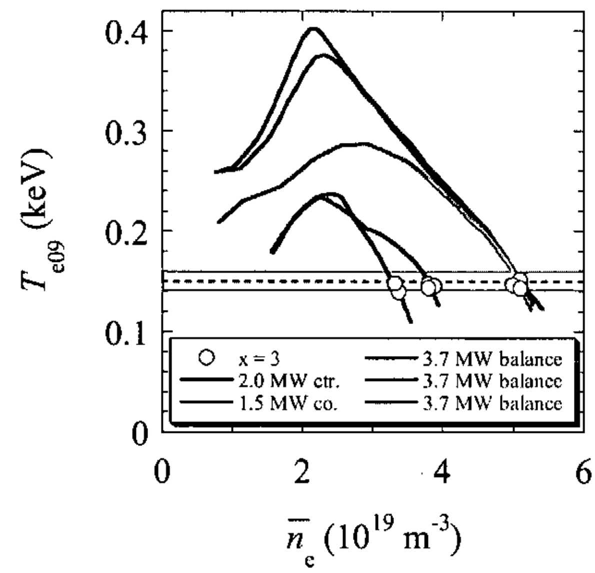

Fig. 2 Edge electron temperature dependence on density for varying input powers.

References
1)Y. Xu *et al.*, Nucl. Fusion **42** (2002) 601.
2) S. Sudo *et al.*, Nucl. Fusion **30** (1990) 11.